Supporting Information:

Supporting information includes the information on atmospheric NO_3^- sampling and analysis, 1 table (Table S1), 4 figures (Figures S1, S2, S3 and S4), and references.

Atmospheric NO_3^- sampling and analysis

For investigating NO_3^- levels in the atmosphere, atmospheric NO_3^-, i.e., both particulate NO_3^- and gaseous HNO_3, was collected along the traverse (coastal Zhongshan Station to Dome A) following similar protocols for previous work in East Antarctica (Savarino et al., 2007; Frey et al., 2009; Erbland et al., 2013). The atmospheric samples were collected on Whatman G653 glass-fiber filters (8 × 10 in; prebaked at 550 ^oC for ~24 hr) using a high volume air sampler (HVAS), with a flow rate of ~1.0 m^3 min^{-1} for 12-15 hr. In total, 34 atmospheric samples were collected on the traverse.

In the laboratory, each filter was cut into pieces using pre-cleaned scissors that were rinsed between samples, placed in ~100 ml of Milli-Q water, ultrasonicated for 40 min and leached for 24 hr under shaking. The sample solutions were then filtered through 0.22 μm ANPEL PTFE filters for NO_3^- concentration analysis.

Ion concentrations (NO_3^- and SO_4^{2-}) in extracted solutions were determined using a Dionex ion chromatograph (ICS 3000) following Shi et al. (2012). Final atmospheric NO_3^- concentrations were normalized to standard temperature and pressure (273 K; 1013 hPa), listed in Table S1.

Table S1 Atmospheric concentrations of NO_3^- and SO_4^{2-} on the traverse from coastal Zhongshan Station to Dome A in East Antarctica.

Sampling location		Atmospheric NO_3^-/ng m^{-3}	Atmospheric SO_4^{2-}/ng m^{-3}
Longitude/^{o} E	Latitude/^{o} S		
76.49	69.79	29	183
76.92	70.64	24	154
77.62	71.5	22	204
77.69	72.37	14	163
77.17	73.15	24	165
76.97	73.86	30	117
76.98	74.9	43	163
76.82	75.87	16	176
77.02	76.86	41	289
77.71	77.15	85	268
76.99	78.36	139	162
77.00	79.01	35	130
77.26	79.82	99	177
77.12	80.42	183	496
77.12	80.42	67	371
77.12	80.42	88	341
77.12	80.42	100	310
77.12	80.42	124	415
77.12	80.42	124	317
77.12	80.42	81	240
77.12	80.42	87	178
77.17	79.63	82	228
77.03	78.77	21	246
77.19	77.83	38	261
77.02	76.74	33	257
77.03	76.42	40	331
76.83	75.87	40	249
76.96	75.03	44	256
77.00	74.09	32	216
76.97	73.86	21	202
77.38	72.84	17	225
77.97	71.93	8	223
77.19	70.97	24	209
76.52	69.97	14	188

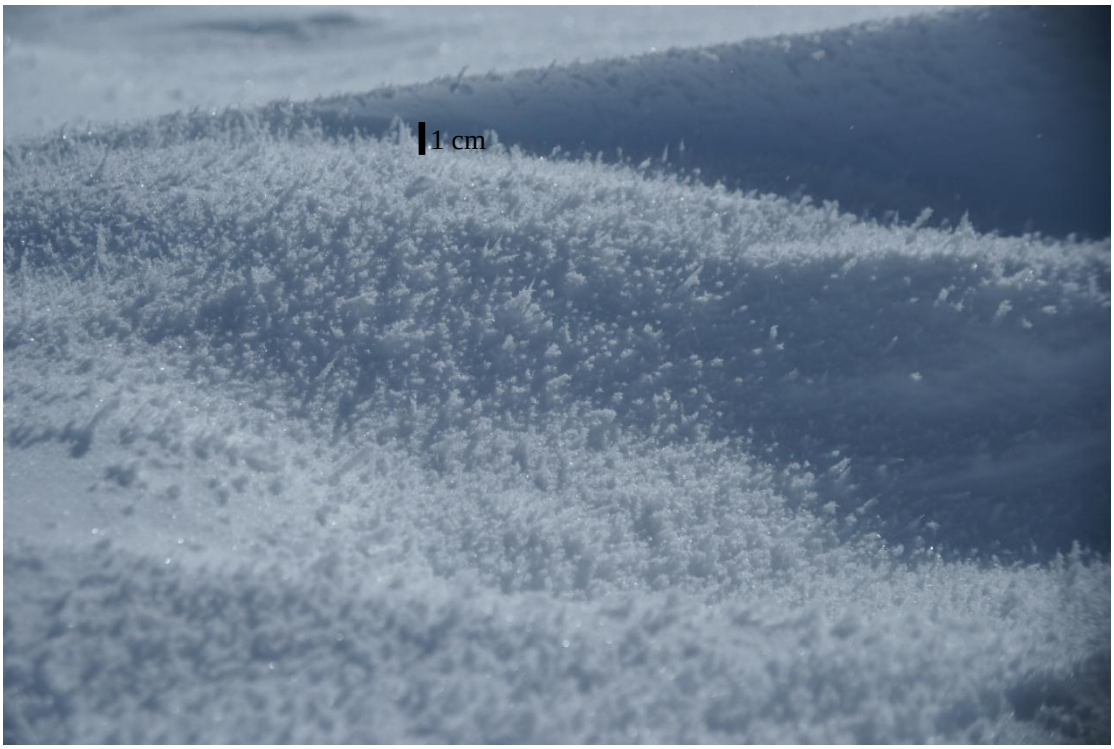

Figure S1 Surface morphology of the surface snow on Dome A plateau, East Antarctica. The needle crystal ice layer is extensively developed. In general, the depth of the crystal layer is < 1.0 cm, and the snowpack is characterized by soft snow texture.

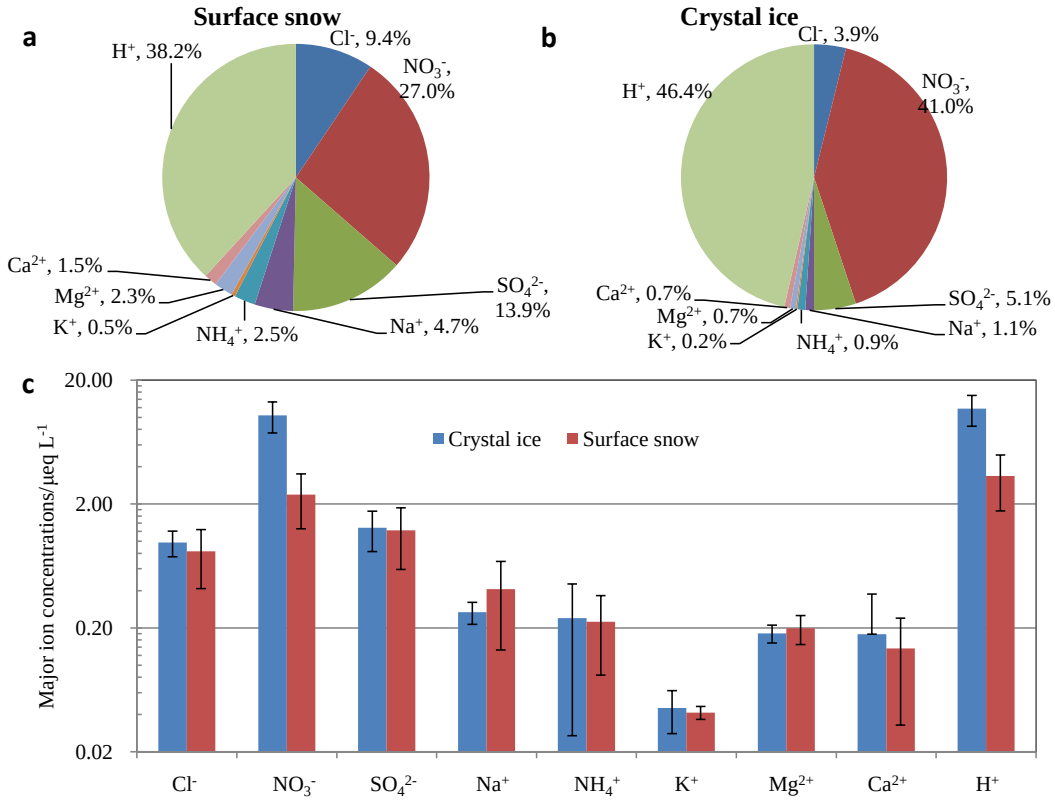

Figure S2 Major chemical ions in surface snow and crystal ice samples on the traverse from coast to the ice sheet summit (Dome A) in East Antarctica. Contribution percentages of each ion to total ion concentrations are shown in (a) and (b), respectively. Concentrations of ions in surface snow and crystal ice are shown in (c), with error bars of one standard deviation (1σ). The concentration of H+ is calculated from the difference between sum anions and sum cations. Note that a base-10 log scale is used for ion concentrations in (c).

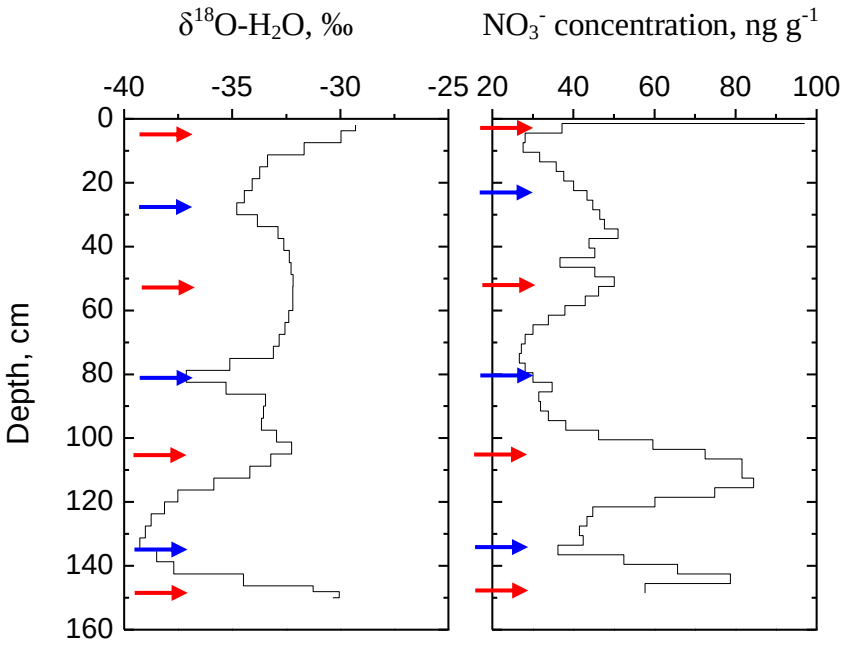

Figure S3 Profiles of $\delta^{18}O$ of H_2O (left panel) and NO_3^- concentration (right panel) in the coastal snowpit SP02. Red and blue arrows represent the middle of the identified warm and cold seasons, respectively. Red solid arrows and blue dashed arrows represent the middle of the identified warm and cold seasons, respectively. One seasonal cycle represents one $\delta^{18}O(H_2O)$ local maxima peak to the next.

Figure S4 Surface morphology of the surface snow at ~600 km from the coast, on the traverse from Zhongshan to Dome A, East Antarctica. The large sastrugi with hard smooth surfaces is extensively developed in this region, mainly formed by wind erosion. The ridges of these sastrugi are typically parallel to the prevailing wind direction.

References

Erbland, J., Vicars, W., Savarino, J., Morin, S., Frey, M., Frosini, D., Vince, E., and Martins, J.: Air-snow transfer of nitrate on the East Antarctic Plateau - Part 1: Isotopic evidence for a photolytically driven dynamic equilibrium in summer, Atmos. Chem. Phys., 13, 6403-6419, doi:10.5194/acp-13-6403-2013, 2013.

Frey, M.M., Savarino, J., Morin, S., Erbland, J., and Martins, J.: Photolysis imprint in the nitrate stable isotope signal in snow and atmosphere of East Antarctica and implications for reactive nitrogen cycling, Atmos. Chem. Phys., 9, 8681-8696, 2009.

Savarino, J., Kaiser, J., Morin, S., Sigman, D.M., and Thiemens, M.H.: Nitrogen and oxygen isotopic constraints on the origin of atmospheric nitrate in coastal Antarctica, Atmos. Chem. Phys., 7, 1925-1945, 2007.

Shi, G., Li, Y., Jiang, S., An, C., Ma, H., Sun, B., and Wang, Y.: Large-scale spatial variability of major ions in the atmospheric wet deposition along the China Antarctica transect (31^{o} N~ 69^{o} S), Tellus B, 64, 17134, doi:10.3402/tellusb.v64i0.17134, 2012.

Zatko, M.C., Geng, L., Alexander, B., Sofen, E.D., and Klein, K.: The impact of snow nitrate photolysis on boundary layer chemistry and the recycling and redistribution of reactive nitrogen across Antarctica and Greenland in a global chemical transport model, Atmos. Chem. Phys., 16, 2819-2842, doi:10.5194/acp-16-2819-2016, 2016.